GMD Integrated Tool (GeoIT): An Integrated Tool for Performing Geomagnetic Disturbance Vulnerability Assessment Studies

Rishi Sharma
EPRI
Palo Alto, CA, USA
rsharma@epri.com

Andres Ovalle
EPRI
Knoxville, TN, USA
aovalle@epri.com

Robert Arritt
EPRI
Knoxville, TN, USA
barritt@epri.com

Thomas J. Overbye
Texas A&M
College Station, TX, USA
overbye@tamu.edu

Arturo Bretas
Sandia Nat. Lab.
Albuquerque, NM, USA
asbreta@sandia.gov

Michael Brown
Pacific Northwest Nat. Lab.
Richland, WA, USA
michael.brown@pnnl.gov

***Abstract*—The impact of geomagnetic disturbances (GMDs) continues to be a significant concern for the North American bulk power system (BPS). In order to assess potential system vulnerabilities and evaluate appropriate mitigation measures, several planning studies must be performed in conjunction, as outlined in the NERC Reliability GMD Vulnerability Assessment Requirement (TPL-007). Presently these studies are conducted across multiple software platforms which requires multiple databases and user intervention. This paper presents a tool that integrates the TPL-007 studies across these multiple platforms, enhancing the accuracy and efficiency of the GMD vulnerability assessment.**

Keywords—Geomagnetic Disturbance (GMD), Geomagnetically Induced Currents (GIC), GICharm, ETTM, B2E, Power System Analysis.

I. Introduction

GMDs occur whenever a large coronal mass ejection—a substantial release of solar energetic particles from the Sun's outer layer—approaches Earth. In these situations, the interaction between the stream of charged particles and the magnetosphere generates significant fluctuations in the ionospheric electric current system near Earth [1]. These fluctuations are characterized by a slowly varying surface magnetic field (geomagnetic field) that induces a surface electric field (geoelectric field) along a conductive loop formed by the Earth's surface and the transmission lines. The resulting geoelectric field induces a voltage in the transmission lines, which drives geomagnetically induced currents (GIC) that flow through the transmission lines and transformer windings to the ground [2].

As GIC are at such low frequencies (50 μHz to 1 Hz), they can essentially be considered quasi-direct current (quasi-DC). These DC currents can lead to part-cycle saturation in high-voltage transformers, potentially resulting in [1]:

- Increased transformer excitation current and increased reactive power losses.
- Increased hotspot heating in transformer windings and structural components occurs when the magnetic flux extends beyond the transformer core [3].
- The transformer to act as a source of both even- and odd-order harmonics, which can lead to either the misoperation or correct operation of protection systems, as well as other impacts on the overall system [4].

The ability to maintain voltage stability during a severe GMD event is a primary concern, not only due to the system-wide increase in transformer reactive power losses but also due to the potential for GMD-related system contingencies. Therefore, to assess potential system vulnerabilities and evaluate appropriate mitigation measures, several planning studies must be performed in conjunction, as outlined in the NERC TPL-007 GMD Vulnerability Assessment [1].

In the currently available commercial and open-source GMD analysis tools, there is limited capability to integrate and automate the computations of the geoelectric field [5], GIC analysis [6], transformer thermal analysis [7] and harmonic computation [4]. Each tool required for these individual computations does not conform to a standardized format for input and output files, making the GMD vulnerability assessment inefficient and cumbersome. The GMD Integrated Tool (GeoIT) automates the workflows of these individual tools across multiple platforms, thereby enhancing the accuracy and efficiency of GMD vulnerability assessments. This paper presents an integrated tool that facilitates GMD analysis and explains how it contributes to a comprehensive GMD vulnerability assessment. In addition to TPL-007 GMD vulnerability assessments, the GeoIT software can also be utilized for model validations, post-event evaluations, and risk assessments.

Section II provides an overview of the modeling considerations for GMD vulnerability assessment. Section III provides an overview of the software platforms used in these assessments, including the GeoIT software. Section IV demonstrates the application of the GeoIT software to perform GMD vulnerability analysis.

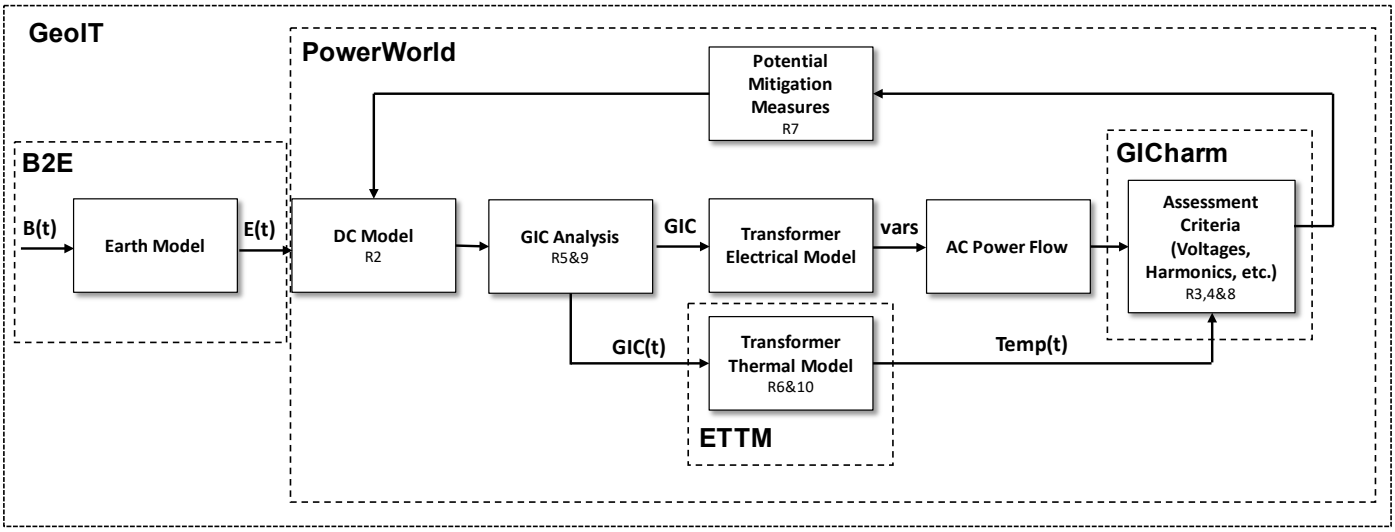

Fig. 1. NERC TPL-007 GMD Vulnerability Assessment Requirement

II. MODELING CONSIDERATIONS

Fig. 1 provides an overview of the requirements for a GMD vulnerability assessment as defined by TPL-007 [8]. The analysis begins with the time-varying geomagnetic field (B(t)) and its interaction with the Earth's conductivity, which produces a surface geoelectric field (E(t)). This geoelectric field serves as an input for the GMD hazard assessment. TPL-007 defines a 1-in-100-year storm in terms of the geoelectric field. Requirement 2 (R2) involves the development of GIC system models (DC models) to enable planners to conduct the necessary studies for completing a GMD vulnerability assessment. Requirements R5 and R9 focus on assessment studies that provide both GIC flows and time-series GIC flows through transformers, which are essential for performing thermal impact assessments (R6 and R10). Requirements R3, R4, and R8 involve assessments of system voltage response and potential voltage stability concerns, using AC load flow studies. These studies must consider GIC-related harmonics in the system response. Requirement R7 pertains to the implementation of potential mitigation options.

A. Geoelectric Field Modeling

The time-varying geomagnetic field (B(t)) induces a surface electric field (geoelectric field) along a conductive loop formed by the Earth's surface and the transmission lines. The geoelectric field time series E(t) (unit: V/m) is computed using the geomagnetic field time series B(t) (unit: nT) and the frequency-dependent magnetotelluric (MT) impedance Z(ω) (unit: (mV/km)/nT), as illustrated Fig. 2.

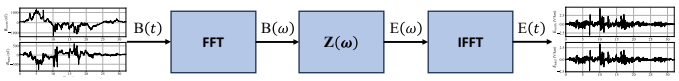

Fig. 2. Computation of the geoelectric field using the geomagnetic field and MT impedance.

First, the spectral estimation of magnetic flux density B(ω), commonly referred to as the magnetic field, is performed using the fast Fourier transform (FFT), as shown in (1). Next, the MT response tensor Z, commonly referred to as MT impedance, is used to obtain the geoelectric field in the frequency domain, as indicated in (2). Finally, the inverse fast Fourier transform (IFFT) is applied to obtain the geoelectric field time series E(t), as shown in (3). In equation (1), (2), and (3), subscripts x and y refer to the north and east directions of the field components, respectively.

$$B_x(\omega) = FFT[B_x(t)],\ B_y(\omega) = FFT[B_y(t)] \tag{1}$$

$$\begin{bmatrix} E_x(\omega) \\ E_y(\omega) \end{bmatrix} = \begin{bmatrix} Z_{xx} & Z_{xy} \\ Z_{yx} & Z_{yy} \end{bmatrix} \begin{bmatrix} B_x(\omega) \\ B_y(\omega) \end{bmatrix} \tag{2}$$

$$E_x(t) = IFFT[E_x(\omega)],\ E_y(t) = IFFT[E_y(\omega)] \tag{3}$$

B. Network Modeling for GIC computation.

To calculate GIC flows required for subsequent planning studies, the planner must create an equivalent DC network based on the associated AC power-flow model for the system, along with additional data not included in standard power-flow models [2]. The GIC flows for the system are typically calculated using commercially available simulation packages.

The GIC computation methodology is detailed in [2]. The induced line voltage V_{dc} is calculated by integrating the surface electric field along the path of the transmission line, as expressed in (4). The equivalent source current I_{Source} is provided in (5). The current injection matrix is derived using the node-arc incidence matrix A and the I_{Source} column matrix, as indicated in (6). Finally, the substation GICs can be determined using I_{inj}, the node admittance matrix Y, and the substation ground resistance R_{gnd} matrix, as indicated in (7).

$$V_{dc} = \int \vec{E} \cdot \vec{dl} \tag{4}$$

$$I_{Source} = V_{dc} / r_{line} \tag{5}$$

$$[I_{inj}] = [A][I_{Source}] \tag{6}$$

$$[GIC] = [R_{gnd}]^{-1}[Y]^{-1}[I_{inj}] \tag{7}$$

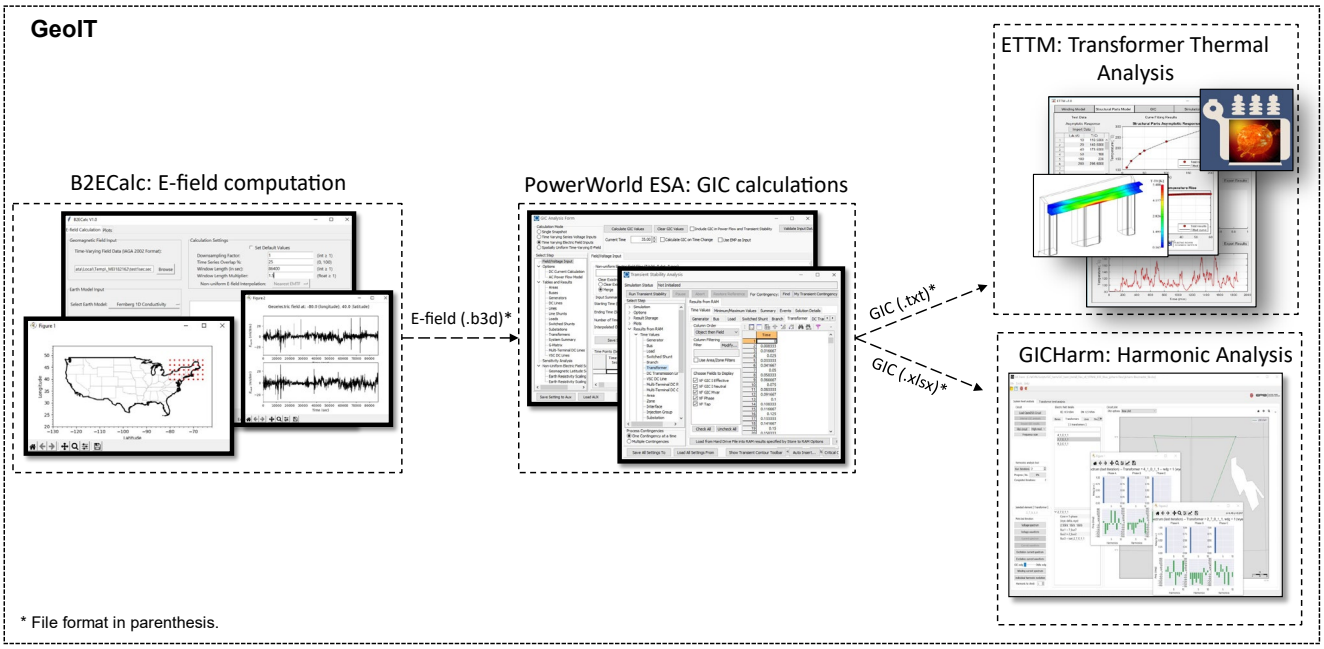

Fig. 3. GeoIT: Integration of B2ECalc, PowerWorld ESA, ETTM, and GICHarm

C. *Transformer Thermal Modeling*

During geomagnetic disturbance (GMD) events, the saturation of the transformer core leads to a significant increase in stray flux, which impinges on the windings and the core's structural components, resulting in hotspot heating within the transformer windings and metallic structural parts. The nonlinear characteristics of the transformer, combined with the frequency dependence of power losses, make the assessment of hotspot heating in transformers a challenging task.

The design of a transformer significantly influences the interaction of stray flux with different transformer components. Therefore, testing is essential to evaluate the thermal response of the transformer. The testing data includes the asymptotic temperature response of the structural part and windings across a range of GIC values, as well as the time-domain temperature rise for a specific GIC reference value.

The transformer thermal modeling methodology is detailed in [7]. Fig. 4 illustrates the thermal model diagram used for estimating transformer hotspots. In this diagram, the ΔT_{asymp} versus GIC lookup table is obtained from the transformer asymptotic response test data. The output of the nonlinear gain block is a weighted GIC time domain signal. The transfer function H(s) is determined using the temperature rise test data at a specified GIC. The output $\Delta\theta_{HS}$ is then added to the oil temperature to calculate the hotspot temperature.

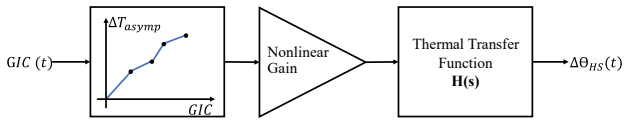

Fig. 4. Thermal model diagram for estimating the temperature rise of hotspots.

Curve fitting is employed to derive the asymptotic temperature rise curve from the ΔT_{asymp} versus GIC lookup table. The asymptotic temperature rise, ΔT_{ultim} for an I_{dc} value that lies between points *m-1* and *m* in the lookup table is represented by (8). For I_{dc} values exceeding the highest GIC in the lookup table, ΔT_{ultim} is calculated using (9).

$$\Delta T_{ultim} = \Delta T_{asymp}(m-1) + \frac{\Delta T_{asymp}(m) - \Delta T_{asymp}(m-1)}{GIC(m) - GIC(m-1)}\left(I_{dc} - GIC(m-1)\right) \quad (8)$$

$$\Delta T_{ultim} = \Delta T_{asymp}(n) + \frac{\Delta T_{asymp}(n) - \Delta T_{asymp}(n-1)}{GIC(n) - GIC(n-1)}\left(I_{dc} - GIC(n)\right) \quad (9)$$

The time-domain temperature rise test data is fitted to an exponential function of the form given by (10), where β, τ_1, and τ_2 are the fitting parameter, the first time constant, and the second time constant, respectively. The transfer function H(s) is obtained from (11) by taking the derivative of the step response (10).

$$\Delta T(t) = \Delta T_{asymp} - \beta\, e^{-\frac{t}{\tau_1}} - \left(\Delta T_{asymp} - \beta\right) e^{-\frac{t}{\tau_2}} \quad (10)$$

$$H(s) = \frac{\beta}{\tau_1 s + 1} + \frac{\Delta T_{asymp} - \beta}{\tau_2 s + 1} \quad (11)$$

D. *Harmonic Modeling*

During a major GMD event, many transformers within a transmission system may become saturated, each injecting high-magnitude harmonic currents. The total distortion current, calculated as the root-sum-square of the harmonic components, injected by a GIC-saturated transformer is comparable in magnitude to its fundamental-frequency reactive current demand. Since the impedance of the transmission system generally increases with frequency (i.e. $X_L = 2*\pi*f*L$), the voltage distortion experienced during a GMD is typically much greater than the fundamental voltage depression caused by reactive demand. The implications of very high harmonic distortion levels during a severe GMD extend well beyond routine power quality considerations, as this distortion can significantly impact system security. The harmonic modeling methodology used in this paper is detailed in [4] and [9].

III. GeoIT: Tool Description

The GeoIT Python package integrates multiple software platforms necessary for conducting GMD vulnerability assessments. Fig. 1 and Fig. 3 illustrate the integration of these tools.

A. B2ECalc: Geoelectric Computation Tool

B2ECalc Python package computes the geoelectric field for the continental United States with minimal user intervention. The only input required is a readily accessible and publicly available geomagnetic field data file in IAGA2002 format. The output file containing the geoelectric field can be seamlessly integrated into commercial software to compute GICs [5].

The tool comes preloaded with three surface impedance and transfer function models: the Fernberg 1D response [10], updated 1D response transfer functions (RTFs) [11] and the non-uniform (3D) response model [12], [13]. To input the geographical locations, the user selects a uniform grid of coordinates, as indicated in Fig. 5. The tool also provides users with the capability to modify the computation algorithm. Users can adjust the input data sampling rate, alter the overlap percentage and length of the time series window for FFT, and change the data padding at both the beginning and end of the time series. The plotting features include time series plots for geomagnetic and geoelectric fields, as well as time-lapse plots for geoelectric field maps. The GeoIT-B2E Python module automates B2ECalc computations in Python.

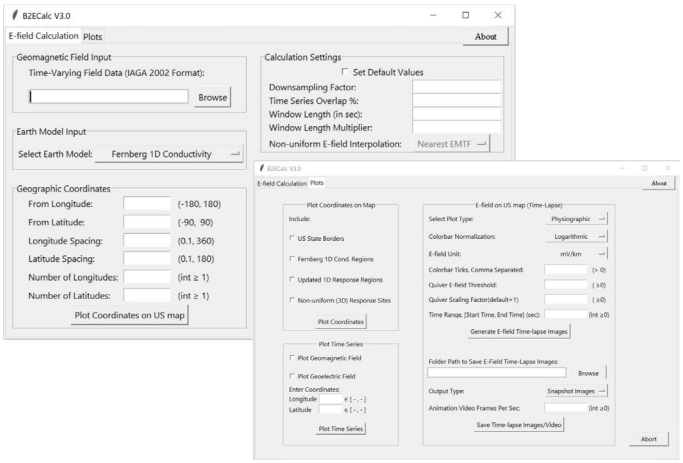

Fig. 5: B2ECalc GUI: geoelectric field computation and plotting tabs.

B. PowerWorld Simulator GIC Computation Tool

The PowerWorld GIC Simulator can utilize the geoelectric field output saved in a B3D file format generated using the B2ECalc tool, to integrate GIC calculations directly within the PowerWorld Simulator. This allows planners to readily assess the impact of GIC on their systems and explore potential mitigation options [6]. The Simulator Automation Server (SimAuto) facilitates the use of PowerWorld functions within Python. The GeoIT-GIC Python module automates GIC computation using the PowerWorld Easy SimAuto (ESA) wrapper. Additionally, the GeoIT-GIC module generates an Excel scenario file that serves as input for GICHarm and produces a text GIC file for ETTM.

C. ETTM: EPRI Transformer Thermal Modeling Tool

The ETTM tool [7] is a thermal transformer model designed to estimate hotspot heating in transformers during GMD events. This thermal model utilizes a transfer function approach.

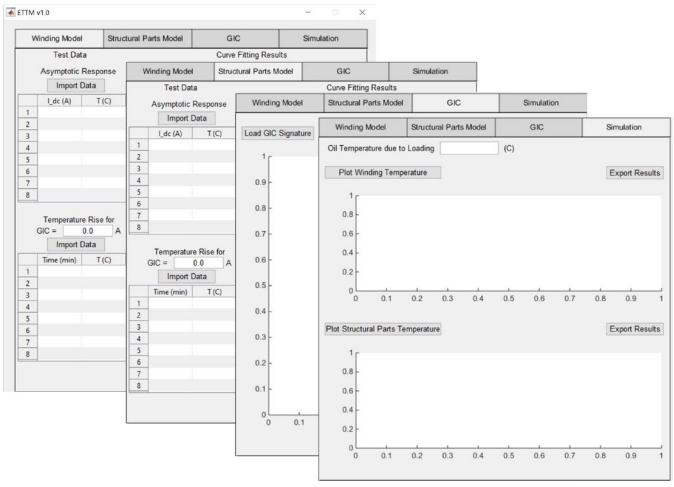

Fig. 6: ETTM GUI: winding model, structural part model, GIC, and simulation tabs.

Fig. 6 illustrates the various tab options available in the ETTM graphical user interface (GUI). In the winding model tab, ETTM utilizes the asymptotic response of transformer windings, along with reference GIC and temperature rise data, to develop the winding thermal model. Similarly, in the structural parts model tab, it employs the asymptotic response of structural parts, along with reference GIC and temperature rise data, to construct the thermal model for the structural parts. The GIC text file generated by PowerWorld ESA is imported through the GIC tab. Finally, temperature plots for both the structural parts and the windings are generated using the simulation tab. The GeoIT-ETTM Python module package automates the computation of the transformer's thermal response by leveraging the ETTM Python package.

D. GICHarm: GIC related Harmonic Analysis Tool.

GICharm [4], [9] is a harmonic assessment tool designed to evaluate the impacts of GMD related distortions. The results of the harmonic assessment must be integrated with fundamental frequency analyses to assess voltage stability during GMD events. The GeoIT-harmonic Python module automates harmonic analysis by utilizing a Python subprocess that employs the GICharm executable, a network model in DSS format, and the GIC scenario file generated by PowerWorld ESA.

IV. Test GMD Event Case Study

To demonstrate the functionality of the integrated tool, a test GMD event profile is applied to the Texas ACTIVSg2000 network, a synthetic grid comprising 2,000 buses [14]. Fig. 7 illustrates the test input geomagnetic field time series, which has a sampling rate of 60 seconds and spans a duration of 30 hours.

Using the GeoIT-B2E module, the geoelectric field time series is computed for the locations indicated in Fig. 8, using

the non-uniform (3D) EMTFs [12], [13]. This uniform grid of geographical coordinates, spaced at one-degree intervals of latitude and longitude, encompasses the entire footprint of the Texas ACTIVSg2000 network. The geoelectric field magnitude time series for the location with the highest geoelectric field magnitude (5.4 V/km) is shown in Fig. 9.

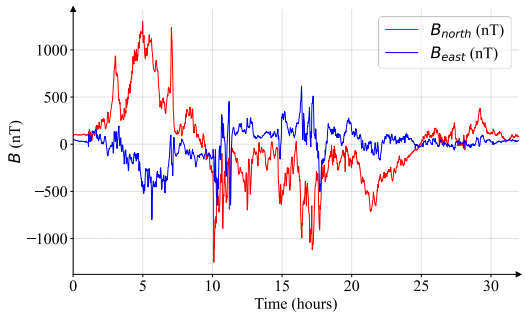

Fig. 7: Time series of the input geomagnetic field, sampled at 60-seconds.

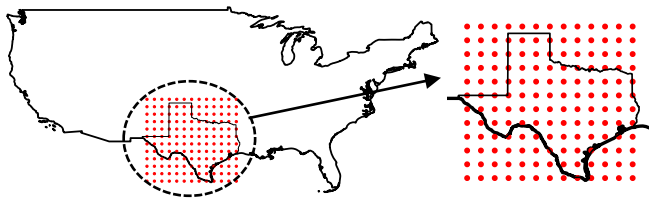

Fig. 8: Geoelectric field computation geographic locations

The geoelectric field map in Fig. 10 shows the magnitude and direction of the field for the selected EMTF sites. This map is generated for the time sample at the 10-hour mark, during which geomagnetic activity peaks.

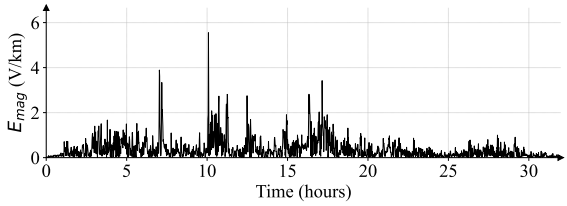

Fig. 9: Geoelectric magnitude time series at longitude -105.2 and latitude 31.6

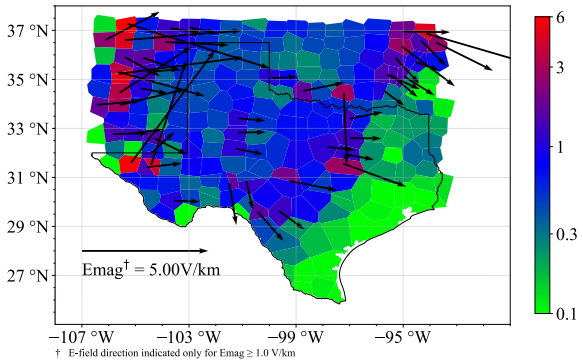

Fig. 10: Map of geoelectric field magnitude (V/km) during peak geomagnetic activity.

Using the GeoIT-GIC Python module, GICs are calculated using geoelectric field data stored in a B3D file format, along with the ACTIVSg2000 network data. The GICs for substations and transmission lines during peak geomagnetic activity at the 10-hour mark are indicated in Fig. 11 and Fig. 12 respectively.

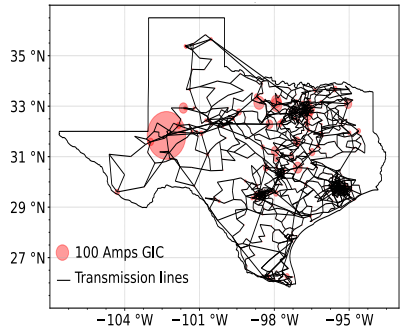

Fig. 11. Substation GICs (Amps) during peak geomagnetic activity.

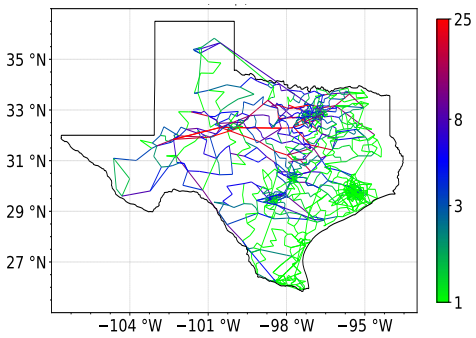

Fig. 12. Line GICs (Amps) during peak geomagnetic activity.

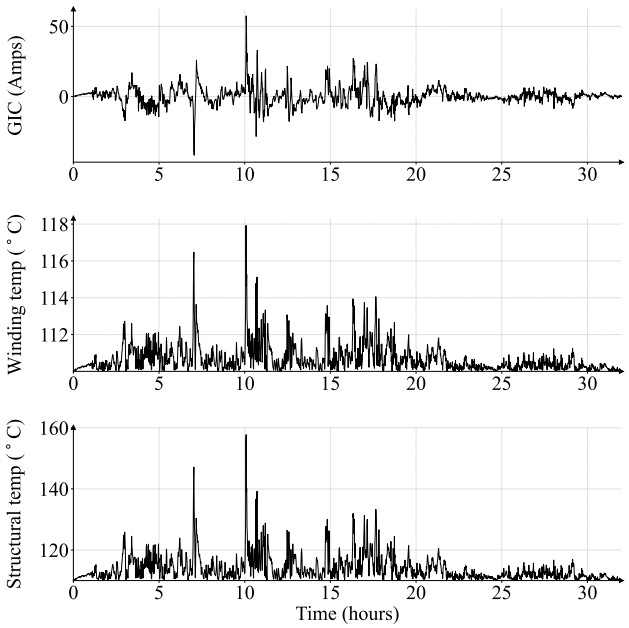

Fig. 13: Thermal analysis results for transformer connecting buses 5045 and 5046 a) Input neutral GICs, b) Winding temperature rise, c) Structural parts temperature rise.

The highest peak neutral GIC value of 57.5 Amps was observed in the transformer connecting buses 5045 and 5046. The GIC time series, winding, and structural part temperature rise for this transformer, calculated using ETTM, is plotted in Fig. 13. With an assumed oil temperature due to loading of 110

℃, the peak winding and structural part temperature were observed to be 117.9 ℃ and 157.8 ℃ respectively.

The GICHarm tool calculates network harmonics by utilizing the network GIC flows for a specified time sample. The selected time sample corresponds to the 10-hour mark, during which geomagnetic activity peaks. For this time sample, the map plot of the voltage total harmonic distortion (VTHD) for phase A is presented in Fig. 14. The VTHD values are observed to be highest at the buses indicated in Table I.

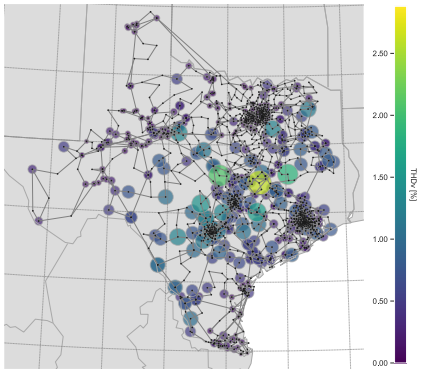

Fig. 14. Percentage of voltage total harmonic distortion (VTHD) for phase A.

Table I
VTHD AT BUSES

Bus	*Ph. A.*	*Ph. B.*	*Ph. C.*
6127	2.6 %	0.8 %	2.6 %
3147	2.0 %	0.5 %	2.0 %
8003	1.8 %	0.4 %	1.9 %

V. CONCLUSIONS

Power systems can be significantly affected by GMD events. The flow of GIC through power transformers is the primary contributor to nearly all GMD-related issues, including the generation of current harmonics, increased reactive power absorption, system voltage instability, and increased hotspot temperatures. To conduct a GMD vulnerability assessment, multiple software platforms are necessary. GeoIT is a tool that seamlessly integrates these various platforms to ensure an accurate and efficient GMD assessment. Using GeoIT, the following GMD vulnerability assessment was demonstrated:

- The computation of the geoelectric field, time series plotting, and geographical visualization were performed using the B2Ecalc Python package.
- GIC computation was performed using PowerWorld ESA. GIC time series plotting, and geographical visualization were conducted using GeoIT plotting features.
- The calculation and plotting of transformer structural part and winding temperatures were performed using the ETTM Python package.
- Harmonic assessment and Voltage Total Harmonic Distortion (VTHD) plotting were performed using GICHarm.

The GeoIT software can also be utilized for model validations, post GMD event assessments, and risk assessments.

ACKNOWLEDGMENT

The authors gratefully acknowledge the support from the U.S. Department of Energy (DoE), Office of Cybersecurity, Energy Security, and Emergency Response (DOE-CESER), Award Number 38601, Pacific Northwest National Laboratory (PNNL), Sandia National Laboratories and EPRI members for the funding of this research. We thank the IRIS DMC for providing online access to EMTF data products. We acknowledge USArray MT, USMTArray-CONUS, and USGS-GEOMAG project efforts that led to the development of EMTFs [12], [13].

REFERENCES

[1] Geomagnetic Disturbance Vulnerability Assessment and Planning Guide. EPRI, Palo Alto, CA: 2024. 3002029754.

[2] North American Electric Reliability Corporation, "Application guide: Computing Geomagnetically-Induced Current in the Bulk-Power System," December 2013.

[3] Transformer Thermal Impact Assessments for DC Withstand Capability: Examining the Impacts of Geomagnetically Induced Current (GIC) on Transformer Thermal Performance. EPRI, Palo Alto, CA: 2019. 3002017708. https://www.epri.com/research/products/0000000030.

[4] Ovalle, R. Dugan and R. Arritt, "GICharm: A System level Analysis tool for Geomagnetic Disturbance related harmonics," 2021 IEEE Industry Applications Society Annual Meeting (IAS), Vancouver, BC, Canada, 2021, pp. 1-7, doi: 10.1109/IAS48185.2021.9677048.

[5] B2ECalc: Geoelectric Field Computation Tool Version 2.0. EPRI, Palo Alto, CA: 2023. 3002027073. https://www.epri.com/research/products/000000003002027073.

[6] PowerWorld Geomagnetically Induced Current (GIC) Simulator. https://www.powerworld.com/products/simulator/add-ons-2/simulator-gic.

[7] Geomagnetic Disturbance (GMD) Transformer Thermal Analysis Tool v1.1. EPRI, Palo Alto, CA: 2021. 3002022749. https://www.epri.com/research/products/000000003002022749.

[8] NERC Standard TPL-007-4: Transmission System Planned Performance for Geomagnetic Disturbance Events, North American Electric Reliability Corporation (NERC), Draft 1: March 19, 2020. https://www.nerc.com/pa/Stand/Reliability%20Standards/tpl-007-4.PDF.

[9] Geomagnetically Induced Current Harmonics Tool (GICharm) v6.0: Software Manual. EPRI, Palo Alto, CA: 2024. 3002029748. https://www.epri.com/research/products/000000003002029748.

[10] One-Dimensional Earth Resistivity Models for Selected Areas of Continental United States and Alaska. EPRI, Palo Alto, CA: 2012. 1026430.

[11] Use of Magnetotelluric Measurement Data to Validate/Improve Existing Earth Conductivity Models. EPRI, Palo Alto, CA: 2020. 3002019425.

[12] Schultz, A., Pellerin, L., Bedrosian, P., Kelbert, A., Crosbie, J. (2020-2023). "USMTArray South Magnetotelluric Transfer Functions". doi:10.17611/DP/EMTF/USMTARRAY/SOUTH. Retrieved from the IRIS database on Dec 03, 2024.

[13] Kelbert, A., Kelbert, A., G.D. Egbert and A. Schultz (2011), IRIS DMC Data Services Products: EMTF, The Magnetotelluric Transfer Functions, https://doi.org/10.17611/DP/EMTF.1.

[14] A. B. Birchfield; T. Xu; K. M. Gegner; K. S. Shetye; T. J. Overbye, "Grid Structural Characteristics as Validation Criteria for Synthetic Networks," in IEEE Transactions on Power Systems, vol. 32, no. 4, pp. 3258-3265, July 2017.